

Supporting Information

Subramaniam *et al.* 10.1073/pnas.0710279105

SI Text

Carbon and Nitrogen Fixation. Carbon fixation by *Trichodesmium* was determined by the ^{14}C -uptake method (1) and nitrogen fixation by the C_2H_2 reduction method (2). Carbon fixation by the DDA was measured along with all other phytoplankton and is reported as bulk primary production. Biogenic silica production rates were then used to estimate the productivity of diatoms. *Richelia* N_2 -fixation rates were measured before concentrating samples by either direct collection onto 40- μm Nitex with gentle backwashing into a clean beaker and/or reverse filtration. When colonial *Trichodesmium* was present in the water along with the diatoms, the water was prescreened through a 202- μm mesh to remove it. The concentrate was diluted to a specific volume and checked under a microscope for the presence of other organisms. Samples were assayed by C_2H_2 reduction at the range of irradiances in on-deck incubators (2). We also measured total nitrogen fixation using $^{15}\text{N}_2$ uptake on unscreened volumes of unconcentrated water at select stations. The rates obtained by this technique are highlighted in Table S2 and showed nitrogen-fixation rates at stations dominated by *Richelia* to be as high as $12 \text{ mmol of N m}^{-2} \text{ d}^{-1}$, 10–100 times higher than that obtained by C_2H_2 reduction in this study but comparable with the rates obtained by C_2H_2 reduction without any preconcentration on a previous cruise in 1996 (3). The lower C_2H_2 reduction could be due to the handling required to isolate *Richelia*.

Chlorophyll a. Samples were filtered on to GF/F, 25-mm glass fiber filters and stored in liquid nitrogen. Pigments were separated by a HPLC with a ODS-2 C18 column using a three-solvent gradient system at a flow rate of 1 ml/min. (4).

DIC. A simple conservative mixing model using alkalinity and salinity was developed to calculate the proportions of Amazon

plume water and seawater in a given sample, remove the effects of the river contribution, and calculate the oceanic component (5). The difference between the expected oceanic and observed DIC concentrations was attributed to biological drawdown (6).

Salinity Classification. Although we have used a simple salinity-based classification scheme, the WTNA is an extremely complex and dynamic system with high spatial heterogeneity consisting of eddies, freshwater filaments, and a constantly changing river plume. Instead of a simple seasonal control, surface properties related to the dynamics of the river plume significantly influenced phytoplankton response. Even within the river plume, surface salinity alone was not a perfect predictor of community structure. Because river-borne nutrient concentrations vary with seasonal discharge (7), coastal diatoms and higher NO_3 concentrations could be found at higher salinity (≈ 30 –31) stations in the spring, presumably because of higher initial nutrient concentrations at the river mouth, whereas in the summer, many stations with salinities as low as 28 had no detectable NO_3 and were devoid of coastal diatoms but had relatively high counts of *Trichodesmium*.

Area of the Plume. We used the relationship between salinity and K490, the attenuation coefficient, (8) to calculate the area of WTNA covered by the Amazon River Plume. The area for each month and the corresponding images are provided in Table S1.

Statistics. Matlab Statistical Toolbox was used to perform the Wilcoxon rank sum and Kruskal–Wallis tests. The data for each station of the aggregated parameters in Table 1 are given in Table S2. Systat software was used for the principal-component analysis.

1. Carpenter EJ, Subramaniam A, Capone DG (2004) Biomass and primary productivity of the cyanobacterium, *Trichodesmium* spp., in the tropical N. Atlantic Ocean. *Deep Sea Res* 51:173–203.
2. Capone D, *et al.* (2005) Nitrogen fixation by *Trichodesmium* spp.: An important source of new nitrogen to the tropical and subtropical North Atlantic Ocean. *Global Biogeochem Cycles* 19:doi:10.1029/2004GB002331.
3. Carpenter EJ, *et al.* (1999) Extensive bloom of a N_2 -fixing diatom/cyanobacterial association in the tropical Atlantic Ocean. *Mar Ecol Progress Ser* 185:273–283.
4. Wright SW, *et al.* (1991) Improved HPLC method for the analysis of chlorophylls and carotenoids from marine phytoplankton. *Mar Ecol Progress Ser* 77:183–196.
5. Cooley SR, Yager PL (2006) Physical and biological contributions to the western tropical North Atlantic Ocean carbon sink formed by the Amazon River plume. *J Geophys Res* C 111, doi:10.1029/2005JC002954.
6. Cooley SR, Coles VJ, Subramaniam A, Yager PL (2007) Seasonal variations in the Amazon plume-related atmospheric carbon sink. *Global Biogeochem Cycles* 21, doi:10.1029/2006GB002831.
7. DeMaster DJ, Aller RC (2001) Biogeochemical Processes on the Amazon Shelf: Changes in Dissolved and Particulate Fluxes During River/Ocean Mixing. in *Biogeochemistry of Major World Rivers*, eds Degens ET, Kempe S, Richey JE (Wiley, New York), pp 323–347.
8. Del Vecchio R, Subramaniam A (2004) Influence of the Amazon River on the surface optical properties of the western tropical North Atlantic Ocean. *J Geophys Res* 109, doi:10.1029/2004JC002503.

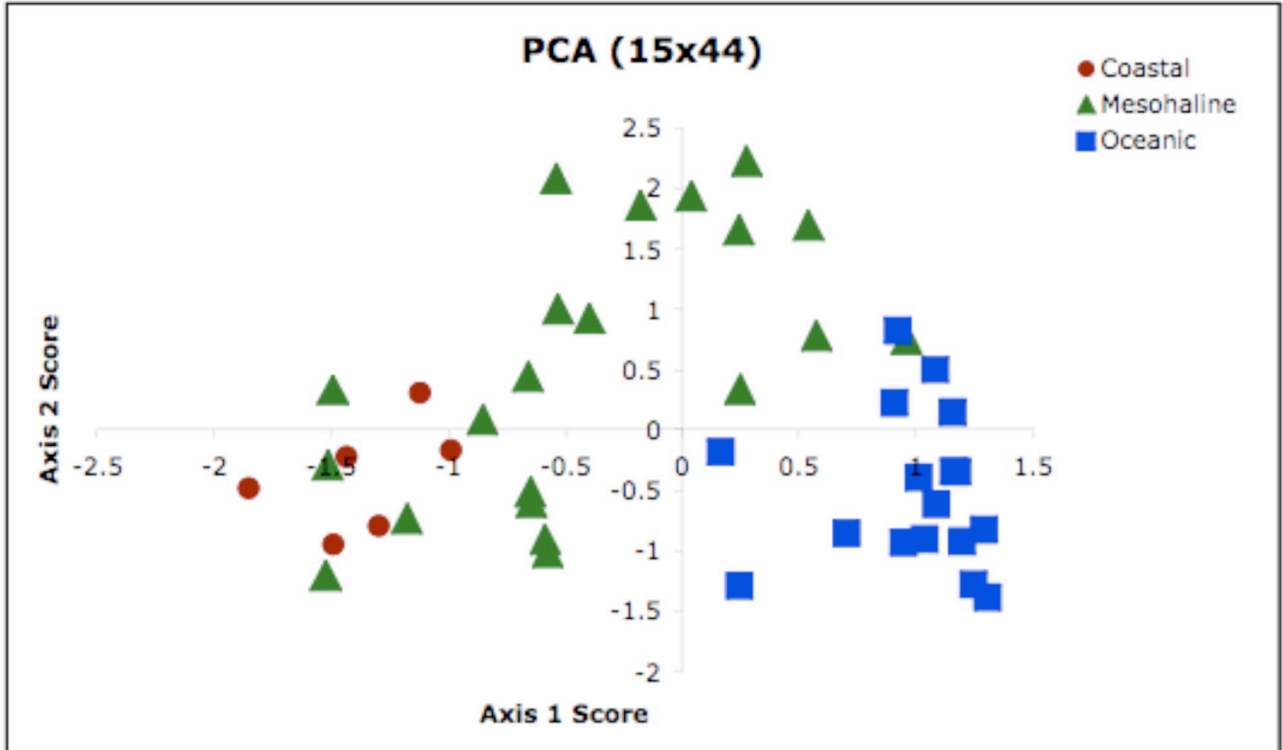


Fig. S1. Component loading scores for the first (x) and second (y) axes of the PCA for each station. The x axis describes the coastal–oceanic gradient, with the coastal stations having a negative score, whereas the oceanic stations have a positive score. The y axis describes the DDA blooms, stations with high *Richelia*, N_2 fixation rates, and low DIC have positive scores.

Table S1. Area of the Amazon River plume as detected by SeaWiFS K490 monthly climatology

Month	km ²	m ²	mol/month
January	294,435	2.9E+11	5.9E+10
February	297,675	3.0E+11	6.0E+10
March	361,341	3.6E+11	7.3E+10
April	705,267	7.1E+11	1.4E+11
May	1,053,000	1.1E+12	2.1E+11
June	1,283,445	1.3E+12	2.6E+11
July	1,307,907	1.3E+12	2.6E+11
August	1,232,820	1.2E+12	2.5E+11
September	885,897	8.9E+11	1.8E+11
October	490,941	4.9E+11	9.9E+10
November	277,101	2.8E+11	5.6E+10
December	252,963	2.5E+11	5.1E+10

Total annual new carbon (mol/yr): $1.7 \pm 0.6 \text{ E} + 12$.

Table S3. A principal-component analysis (performed on log+1 transformed data) was applied on data from the 44 stations where every one of 15 key variables (listed below) were measured

	Axis 1	Axis 2	Axis 3	Axis 4
%VAR EXP:	35	19	13	7
MLD	0.901	-0.218	-0.238	-0.034
TEMP	-0.866	0.066	0.243	0.147
SAL	0.844	-0.016	0.081	-0.150
LIGHT	0.798	-0.386	0.322	0.072
DSI	-0.767	-0.327	0.069	0.226
WIND	0.715	0.293	-0.219	-0.099
CHLA	0.655	0.393	0.093	0.196
RICHEL	-0.003	0.913	-0.020	0.105
N2FIX	0.239	0.748	0.399	-0.047
DICR	0.454	-0.633	0.170	0.288
SRP	0.375	0.204	-0.772	0.055
TRICHO	0.156	0.318	0.734	-0.387
BSI	-0.430	0.467	-0.516	0.061
PRIMPROD	0.474	0.166	0.137	0.727
DFE	-0.127	0.277	0.281	0.428

The PCA generated four axes that explained 74% of the system variance. Axis 1 (35%) described the river–ocean gradient correlated with mixed layer depth (MLD), sea surface temperature (TEMP), sea surface salinity (SAL), 1% light depth (LIGHT), dissolved silicon (DSI), wind speed (WIND), and chlorophyll a (CHLA). Axis 2 (19%) described the mesohaline DDA blooms and correlated with integrated *Richelia* abundance (RICHEL), river-corrected DIC (DICR), integrated N₂ fixation (N2FIX). Axis 3 (13%) correlated with integrated *Trichodesmium* abundance (TRICHO), surface soluble reactive phosphorus (SRP), and integrated biogenic silica (BSI). The fourth axis (7%) correlated with total integrated primary production (PRIMPROD) and dissolved iron (DFE), suggesting that iron was not limiting production in this region. The correlations shown are the component loadings from SYSTAT, i.e., the correlation of each variable to the component axis. The key result is that the largest nonconservative changes in DIC and nitrogen-fixation rates are associated with high *Richelia* biomass on Axis 2. PCA was conducted by using SYSTAT.

Other Supporting Information Files

[Table S2 \(XLS\)](#)